

Constrained Prescriptive Trees via Column Generation

Shivaram Subramanian*, Wei Sun*, Youssef Drissi, Markus Ettl

IBM Research, Yorktown Heights, NY 10591, USA
subshiva, sunw, youssefd, mettl@us.ibm.com

Abstract

With the abundance of available data, many enterprises seek to implement data-driven prescriptive analytics to help them make informed decisions. These prescriptive policies need to satisfy operational constraints, and proactively eliminate rule conflicts, both of which are ubiquitous in practice. It is also desirable for them to be simple and interpretable, so they can be easily verified and implemented. Existing approaches from the literature center around constructing variants of prescriptive decision trees to generate interpretable policies. However, none of the existing methods are able to handle constraints. In this paper, we propose a scalable method that solves the constrained prescriptive policy generation problem. We introduce a novel path-based mixed-integer program (MIP) formulation which identifies a (near) optimal policy efficiently via column generation. The policy generated can be represented as a multiway-split tree which is more interpretable and informative than a binary-split tree due to its shorter rules. We demonstrate the efficacy of our method with extensive experiments on both synthetic and real datasets.

Introduction

With the abundance of available data, many enterprises seek to implement data-driven prescriptive analytics to help them make better decisions. Unlike *predictive* analytics, which applies mathematical models to forecast potential outcomes, *prescriptive* analytics determines the best course of action for the future, frequently utilizing the outcome of a predictive model (Lepenioti et al. 2020). For instance, in revenue management, pricing decisions are based on estimated demand learnt from historical sales data; in healthcare, personalized medicine is prescribed based on past patients' responses towards different treatment options. A key characteristic of prescriptive analytics is the presence of constraints, which is largely missing from predictive analytics. Constraints are ubiquitous in practice: a revenue-maximization problem may limit prices such that the resulting demand does not exceed production capacity; similarly, a patient's available treatment options may be limited by his or her pre-existing conditions.

Despite machine learning (ML) making huge strides in recent years, there are several obstacles standing in the way

of widespread adoption of prescriptive analytics in practice. Firstly, prescriptive analytics often works in conjunction with predictive models, whose output may be nonlinear, non-convex and/or discontinuous (and therefore not differentiable), resulting in intractable downstream optimization problems. To generate meaningful policies, it is critical to embed the myriad of business requirements into the decision optimization problem, exacerbating the computational challenge at hand. Secondly, powerful black-box predictive models inevitably obscure the downstream decision-making process, making it difficult for enterprises to understand and trust the prescribed policies. Meanwhile, recommendations based on these models tend to be highly complex, making implementation and maintenance of these policies challenging and cumbersome.

There have been some recent works studying the problem of generating interpretable prescriptive policy. A common theme is to construct variants of decision trees which represent the prescribed policies, as trees provide “human-friendly” explanations (Frosst and Hinton 2017, Miller 2019). Each path in a tree from the root node to a leaf node corresponds to a policy, and all samples in a leaf are prescribed with a same action. The procedure of generating such a tree-based policy may vary - the prediction step can be either embedded in the policy generation step (Kallus 2017, Bertsimas, Dunn, and Mundru 2019), or explicitly separated from prescription (Zhou, Athey, and Wager 2018, Amram, Dunn, and Zhuo 2020, Biggs, Sun, and Ettl 2021). Meanwhile, the prescriptive tree can be constructed either greedily (Zhou, Athey, and Wager 2018, Biggs, Sun, and Ettl 2021) or optimally (Kallus 2017, Amram, Dunn, and Zhuo 2020). However, none of the existing methods are capable of handling operational constraints which are paramount for successful enterprise adoption of prescriptive analytics - this is the gap which we intend to fill with this work.

In this paper, we propose a scalable method to solve the constrained prescriptive policy generation problem. We consider the *predictive teacher* and *prescriptive student* framework [Zhou, Athey, and Wager 2018, Amram, Dunn, and Zhuo 2020, Biggs, Sun, and Ettl 2021], where a predictive model (teacher) is first trained to produce counterfactual outcomes associated with different actions for every sample in the dataset. Based on the counterfactual estimations, the downstream prescriptive model (student) determines the

*These authors contributed equally.

best set of policies to divide the samples that optimizes the given objective. Our key contributions are as follows:

1. Constrained policy prescription To the best of our knowledge, we are the first to propose a prescriptive tree which is capable of handling constraints that span across multiple rules. Existing tree-based approaches in the literature typically produce unconstrained policies that ignore rule conflicts and operational feasibility, severely limiting their usefulness in practice.

2. Novel MIP formulation We model rules or paths in a tree explicitly as it provides a natural way to impose constraints unlike prior MIP methods which rely on arc-based feature-level models. More specifically, we show that the constrained tree-based policy prescription problem can be formulated as a set-partitioning problem with side-constraints. A key challenge here is that the search space for rules may be computationally prohibitive to solve the problem directly for high dimensional datasets. To overcome this hurdle, we implement column generation [Ford Jr and Fulkerson 1958], where promising candidate rules can be generated dynamically. Column Generation (CG) can be applied as an exact method as well as an efficient technique to obtain near-optimal solutions in practical settings.

3. Scalable algorithm The aforementioned *path-based* MIP formulation enables breakthroughs in scalability over prior *arc-based* MIP decision tree methods (e.g., Bertsimas, Dunn, and Mundru 2019, Amram, Dunn, and Zhuo 2020), which suffer from a scalability issue as their formulation requires $O(2^k M)$ binary variables where k and M refer to the depth of the tree and the number of samples respectively. In contrast, the number of binary decision variables in our MIP formulation is independent of the sample size and equals the number of candidate decision rules. While this number can also be prohibitive in the worst case, we only need to generate candidates as needed to find a near-optimal solution and typically the resultant number of candidate rules is far less than the number of possible rules. As a result, while existing approaches struggle to process datasets beyond 10^5 samples and depth 2, a first crude implementation of our proposed CG heuristic algorithm handles 10^6 samples at a depth equivalent of 5, with the potential to solve larger datasets using more efficient implementations.

4. More interpretable policies Contrary to the existing tree-based methods which typically construct a binary-split tree where each node has at most two children, we consider a multiway-split tree, where a node may have more than two child nodes (refer to Figure 1b for an example). Multiway trees offer the advantage over binary trees that an attribute rarely appears more than once in any path from root to leaf, which are easier to comprehend than its binary counterparts (Fulton, Kasif, and Salzberg 1995).

5. Extensive numerical results We perform extensive experiments to show that the proposed approach produces solutions of superior quality compared to prior prescriptive tree approaches in the literature. We present several use cases with public datasets to demonstrate our method’s flexibility in handling a variety of constraints.

Related Literature

There has been a surge of interest in making ML models more interpretable in the recent years (e.g., Ribeiro, Singh, and Guestrin 2016, Lundberg and Lee 2017, Guidotti et al. 2018, Carvalho, Pereira, and Cardoso 2019). A common framework used to gain interpretability is *knowledge distillation* (Hinton, Vinyals, and Dean 2015), where a complex model serves as a teacher and a simpler model learns to mimic the teacher as a student. For instance, this concept has been implemented in explainable reinforcement learning (XRL) [Liu et al. 2018, Puiutta and Veith 2020], where a black-box teacher model first learns the policies, then a regression tree is trained to approximate these policies. A notable distinction of the framework considered in this work lies in the different roles played by the teacher and the student models. More specifically, in our setting, the prescriptive student does not merely replicate the teacher’s behavior, rather it determines the optimal policies. Meanwhile, the teacher in our framework does not produce policy, rather it provides the counterfactual estimations which guide the student in determining the optimal policies.

As this framework explicitly decouples prediction from prescription, one can take advantage of the latest advances in ML and utilize powerful models such as boosted trees or deep neural networks for the prediction task. It is in contrast to an alternative approach, i.e., embedding prediction inside prescription by combining the tasks of estimating a predictive model and learning the optimal policy (Kallus 2017, Bertsimas, Dunn, and Mundru 2019). While this approach offers the benefit of learning prediction and prescription from data in a single step, it also limits the predictive models to piecewise-constant or piecewise-linear functions for computational tractability. Such restriction may lead to severe model misspecification when the underlying structure of the outcome takes a more complex form.

Besides the aforementioned interpretable prescription methods, there exist approaches from causal analysis, where the focus is on estimating heterogeneous treatment effects which can in turn quantify the impact of prescribing actions (e.g., Shalit, Johansson, and Sontag 2017, Wager and Athey 2018, Künzel et al. 2019). These methods are typically limited to binary actions and are less concerned with interpretability.

Decision trees have been used extensively in machine learning, mainly due to their transparency which allows users to derive interpretable results (Zhu et al. 2020). As learning an optimal decision tree is NP-complete (Laurent and Rivest 1976), popular algorithms such as CART (Breiman et al. 1984) have relied on greedy heuristics to construct trees. Recent advances in modern optimization have facilitated a nascent stream of research that leverages mixed-integer programming to train globally-optimal trees (e.g., Bertsimas and Dunn 2017, Bertsimas, Dunn, and Mundru 2019, Aghaei, Azizi, and Vayanos 2019, Aghaei, Gomez, and Vayanos 2020, Zhu et al. 2020). In particular, Bertsimas, Dunn, and Mundru 2019 and Amram, Dunn, and Zhuo 2020 have applied this MIP approach to learn a prescription policy. Notable differences between our work and the aforementioned MIP approach are 1) instead of construct-

ing a binary-split tree, we construct a multiway-split tree which is more interpretable (Fulton, Kasif, and Salzberg 1995). 2) Instead of an arc-based formulation, we present a path-based MIP formulation to construct the tree, which allows us to model constraints naturally and solve the problem efficiently via column generation (CG). CG has been successfully adopted by the AI community (e.g., Bach 2008, Jawanpuria, Nath, and Ramakrishnan 2011) and in practice to solve complex discrete optimization models including airline scheduling (Klabjan et al. 2002, Subramanian and Sherali 2008, Bront, Méndez-Díaz, and Vulcano 2009), vehicle routing (Chen and Xu 2006), and inventory planning for supply chain, among others (Desaulniers, Desrosiers, and Solomon 2006, Xu 2019).

Problem Formulation

Predictive Teacher with Prescriptive Student Tree

We assume there are M observational data samples $\{(x_i, \pi_i, y_i)\}_{i=1}^M$, where $x_i \in \mathcal{X}^d$ are features, π_i refers to the action chosen from a discrete set Π , and y_i is the uncertain quantity of interest, which can be a discrete label for classification or a continuous quantity for regression. In a use case of pricing studied in Section , x_i represents customer features, π_i is the price of a product and $y_i \in \{0, 1\}$ indicates whether the product was sold (1) or not (0). In another use case on housing upgrade, x_i represents attributes associated with a house, π_i is the construction grade which a builder can choose from, and y_i indicates the sale price of a house.

As a standard practice in causal inference literature, we make the ignorability assumption (Hirano and Imbens 2004), i.e., there were no unmeasured confounding variables that affected both the choice of decision and the outcome.

We assume an underlying function $f : \mathcal{X}^d \times \Pi$ which maps the features and an action to the outcome y . An optimal policy selects an action $\tau^*(x)$ for each sample based on its features to maximize the objective function:

$$\tau^*(x) = \arg \max_{\pi \in \Pi} g(f(x, \pi)) \quad (1)$$

In pricing, $f(x, \pi)$ represents the probability of purchase given price π and customer feature x , while $g = \pi f(x, \pi)$ denotes the expected revenue.

In reality, the true response function $f(x, \pi)$ is unknown, but can be estimated. We refer to the proxy response function \hat{f} as the teacher model. There are many possible choices for \hat{f} . Biggs, Sun, and Ettl 2021 learn a teacher model by solving an empirical risk minimization problem. Zhou, Athey, and Wager 2018, Amram, Dunn, and Zhuo 2020 use doubly-robust estimators to estimate the counterfactual outcomes (Dudík, Langford, and Li 2011). The advantage of separating the prediction task from prescription is that one has the flexibility to choose the “best” counterfactual inference model available as the teacher for a given application.

If we substitute the proxy response function \hat{f} into the optimization problem in (1), the prescription problem is reduced to enumerate through Π to determine the optimal policy. More concretely, we use $g_{i,\pi}$ to denote the estimated

counterfactual outcome by the teacher model for a given action π , i.e., $g_{i,\pi} = g(\hat{f}(x_i, \pi))$, and the policy prescription problem becomes

$$\tau(x) = \arg \max_{\pi \in \Pi} \sum_{i=1}^M g_{i,\pi}$$

Note that since $g_{i,\pi}$ is just an input to the downstream optimization problem, the task of policy prescription becomes much simpler, i.e., for each sample i , enumerate through $g_{i,\pi}$ and select the best action. One caveat of this approach is that the resulting policy may be too complex when the action space is huge, and may not offer any insight into how the prescription is made.

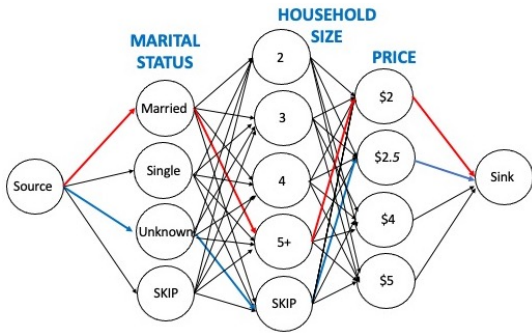
To aid interpretability, we restrict the policy to a certain class of prescriptive models. A common choice in the literature is a binary-split decision tree of a pre-specified depth k , $\mathcal{T}_b(k)$, which has at most 2^k leaves (e.g., Biggs, Sun, and Ettl 2021, Amram, Dunn, and Zhuo 2020). In this work, we consider a multiway-split tree (MT) as the prescriptive student model, denoted as $\mathcal{T}_m(n)$, where n indicates the number of leaves. An example of a MT with $n = 8$ is shown in Fig 1b. A MT with n leaves $\mathcal{T}_m(n)$ is comparable to a binary-split tree grown to its full width with the same number of leaves, i.e., $\mathcal{T}_b(k)$ where $2^k = n$. We refer to our model as *student prescriptive multiway-split tree* problem, or SPMT,

$$\text{(SPMT)} \quad \max_{\tau(x) \in \mathcal{T}_m(n)} \sum_{i=1}^M g_{i,\pi} \quad (2)$$

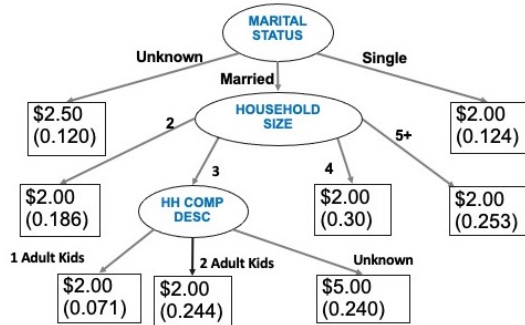
There are many real-life situations where a decision maker may only want to use a subset of features \hat{x} to define a policy. For instance, one may not want to include personal features due to privacy and fairness concerns. This highlights another advantage of the *prescriptive knowledge distillation* framework - an “informative” teacher which is trained on all available data provides accurate estimates on the counterfactuals and guides a student model which uses fewer features. To avoid overloading notations, in the remainder of the paper, we assume x^d are d categorical features that can be accessed by the student model. Our method can also be applied to numerical features that are discretized, as shown in the experiments in Section . More discussions can be found in the supplementary material.

Decision Rule Space

The high level idea of our approach is to identify n decision rules from a potentially huge rule space, which contains every possible combination of input features for policy prescription. To model this, we construct a feature graph, where each decision rule is mapped to a distinct, independent path in the graph. Specifically, we consider an acyclic multi-level digraph, $G(V, E)$, where each feature indicates a level in the graph, represented by multiple nodes corresponding to its distinct feature values. Nodes of one feature are fully connected to nodes in the next level. V also contains a source and sink node. In addition, a unique and critical characteristic of G is that for each feature, with the exception of the action nodes π , we introduce a dummy node *SKIP*. Fig 1a



(a) Feature graph with 3 features including action (price)



(b) A multiway-split tree with $n = 8$ rules

Figure 1: A sample output from the grocery pricing use case

illustrates an example of a feature graph with three features, including the action nodes.

A decision rule is defined as a path $P \in \mathcal{P}$ from the source to the sink node on G . A path passing through a *SKIP* node excludes the corresponding feature from the decision rule. As *SKIP* nodes allow paths to ignore features, paths on this acyclic graph represent all possible feature combinations, defining the full decision rule set \mathcal{P} that one has to enumerate through to solve the policy prescription problem. In the rest of the paper, we use paths and rules interchangeably.

Proposition 1 $|V|$ is linear in d . $|\mathcal{P}|$ is exponential in d .

The space for decision rules expands dramatically for high-dimensional datasets and enumerating \mathcal{P} becomes intractable. We present an algorithm which searches through the space efficiently in Section , by solving linear programs (LP) and dynamically generating paths when needed.

So far, we have described our approach of policy prescription as a rule selection problem, whereas the SPMT problem in (2) restricts the policy to be a multiway-split tree $\mathcal{T}_m(n)$. There is a key distinction between a set of decision rules and a tree: the former is viewed as unordered rules which may overlap, whereas a tree has a hierarchical structure which ensures rules are non-overlapping, i.e., each example is covered by exactly one rule (Fürnkranz 2017). In the next section, we will introduce a MIP formulation to ensure the sample-level non-overlapping condition will be satisfied by the prescribed rules. Note that while the arrangement of features in G is not relevant to the objective value of

(2), it does affect interpretability. Hence, we utilize insights from the teacher model and arrange the features based on their importance (e.g., Lundberg and Lee 2017) when constructing G (see an example presented in the supplementary material).

Set Partitioning Problem

We now present a novel path-based MIP formulation to select a subset of n rules from a feature graph. We denote decision rule as $j = 1, \dots, N$, where $N = |\mathcal{P}|$. Let $S_j \in [M]$ be the subset of observations which fall into rule j . Every sample in S_j is prescribed with a same action $q_j \in \Pi$. Let z_j be a binary decision variable which indicates whether rule j is selected (1) or not (0), for $j = 1, \dots, N$. We would like to enforce that each sample i is only assigned to a single rule, and failure to comply with the condition incurs a positive cost $c_i = c$ for all i . Define r_j as the expected outcome associated with rule j , i.e., $r_j = \sum_{i \in S_j} g_{i, q_j}$. The *set partitioning problem* (SPP) which identifies n out of N decision rules can be written as follows,

$$\max \sum_{j=1}^N r_j z_j - \sum_{i=1}^M c_i s_i$$

$$\text{s.t.} \sum_{j=1}^N a_{ij} z_j + s_i = 1, \quad \forall i = 1, \dots, M \quad (3)$$

$$\sum_{j=1}^N z_j \leq n \quad (4)$$

$$z_j \in \{1, 0\}, \quad \forall j = 1, \dots, N$$

$$s_i \geq 0, \quad \forall i = 1, \dots, M$$

where $a_{ij} = 1$ if sample i satisfies the conditions (features) specified in rule j , and 0 otherwise. While a sample may fall into several rules, the set partitioning constraint (3) along with the non-negative slack variables s_i that are included with a sufficiently large penalty c_i , ensure that each sample is ultimately covered by exactly one rule. Cardinality constraint (4) ensures that at most n rules are active in the optimal solution \mathbf{z}^* , where n is a user defined input corresponding to 2^k leaf nodes in a binary-split tree of depth k .

Theorem 1 Active paths in \mathcal{P} which are identified by \mathbf{z}^* correspond to an optimal solution $\mathcal{T}_m^*(n)$ in SPMT.

We have shown that if we can solve SPP, then we have identified a multiway-split tree with n rules. It is well-known that SPP is NP-Hard (Wolsey and Nemhauser 1999). Nevertheless, (near) optimal or high quality feasible solutions can be obtained in practice for moderate sized instances (Atamtürk, Nemhauser, and Savelsbergh 1996). Unfortunately, in our case, the cardinality of feasible rules may become prohibitive to solve it directly. We will now present an efficient algorithm to overcome this hurdle.

An Efficient and Scalable Algorithm

The technique of column generation (CG) is used for solving linear problems with a huge number of variables for which it

is not practical to explicitly generate all columns (variables) of the problem matrix. More specifically, we consider a *restricted master problem* (RMP) version of SPP, where we 1) consider only a subset of paths, \hat{N} , where \hat{N} is typically much smaller than N , and 2) relax the integrality constraints on z_j to $0 \leq z_j \leq 1$ for all $j = 1, \dots, \hat{N}$.

Denote the dual variables associated with the set partitioning constraints in (3) and the cardinality constraint in (4) as λ_i and μ respectively. The dual formulation of RMP can be found in the supplementary material. In particular, the dual feasibility constraint corresponding to path j is given by

$$\sum_{i=1}^M a_{ij} \lambda_i + \mu \geq r_j, \quad \forall j = 1, \dots, \hat{N} \quad (5)$$

From (5), we can derive the reduced cost for path j as

$$rc_j = r_j - \left(\sum_{i=1}^M a_{ij} \lambda_i + \mu \right). \quad (6)$$

Additional constraints are handled in (6) similar to the partitioning and cardinality restrictions via their corresponding dual variables.

The key idea of CG is as follows - as we solve a much smaller RMP to optimality, dual feasibility is guaranteed only for the rules included in \hat{N} and we must verify that the dual feasibility are also satisfied by the rules not included in the RMP. A path violating the dual constraint (5) has a positive reduced cost and must be added to the RMP. Therefore, we identify paths that maximally violate Eq (5), i.e., $\max rc_j$ or $\min -rc_j$. The implicit search for K paths having the highest reduced cost amounts to optimizing a *sub-problem*, which is a *K-shortest path problem* (KSP) over G (Horne 1980, Irnich and Desaulniers 2005), where the cost on a path is the negative of its reduced cost defined in (6). The CG procedure converges to an optimal solution of the LP relaxation of SPP when dual feasibility is achieved, i.e., $rc_j \leq 0$ for all $j = 1, \dots, N$. Otherwise, new paths are found and their corresponding columns A_j which comprise of coefficients a_{ij} are added to RMP, which is re-optimized. We repeatedly solve RMP and KSP until successive dual solutions converge or we reach a maximum iteration limit.

Once the CG procedure has converged, we reimpose the binary restrictions on \mathbf{z} and solve the resultant Master-MIP. Any of two MIP approaches below can be adopted either individually or in combination depending on the end goal. Since SPP is NP-Hard, obtaining a provably optimal solution may require inordinate run times for challenging instances. For simplicity and replicability, we solve the Master-MIP directly here using a standard optimization library (CPLEX 2020) to distill a (near) optimal subset of prescriptive decision rules. Thereafter, one can optionally switch to the more advanced “branch-and-price” method to converge to an optimal MIP solution [Barnhart et al. 1998].

One common yet critical requirement of prescriptive analytics is to incorporate a myriad of operational constraints. They can be broadly categorized into *intra-rule* and *inter-rule constraints*, which are handled differently in the algorithm.

The scope of *intra-rule constraints* is limited to a single decision rule. They may involve complex path-dependent nonlinear conditions involving several features that cannot be abstracted efficiently into linear constraints. For instance, disallowing certain feature combinations or limiting the number of features. These constraints are easily handled within the KSP subproblem as a feasibility check while extending a partial path to the next node in G (we refer readers to Section 1.2 in Barnhart et al. 1998 for more discussions).

Inter-rule constraints span across many decision rules. One example is the cardinality constraint in (4). Inter-rule constraints can be expressed as linear inequalities in the RMP, which in turn influence the subproblem by modifying the reduced cost. We present detailed use cases in Section along with a house pricing constraint and loyalty pricing implementation in the supplementary material.

Experiments

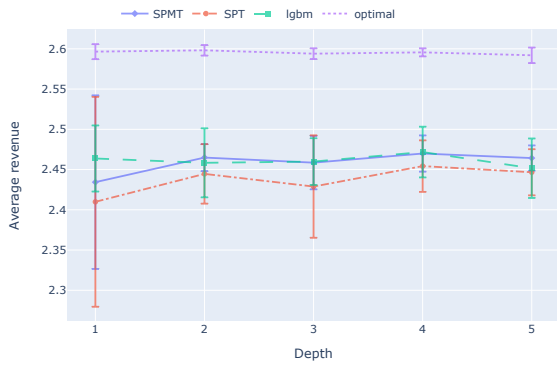
In this section, we perform experiments to demonstrate the efficacy of our method, *Student Prescriptive Multiway-split Tree* (SPMT). We first perform experiments on six simulated datasets which allow us to accurately calculate the resulting outcome. We want to point out that since none of the existing interpretable tree-based methods are capable of handling constraints, we can only benchmark against them in the *unconstrained* setting. Next, we present three use cases with real data as we discuss constrained policy prescription, two of which use publicly available data.

The following baselines are considered: The greedy student prescriptive tree (SPT), is used as the key tree-based prescriptive benchmark since Biggs, Sun, and Ettl 2021 has demonstrated that it outperforms other competing prescriptive tree methods (i.e., Kallus 2017, Athey and Imbens 2016). A true optimum policy (OPTIMAL) which can be found by identifying the price which results in the highest revenue according to the underlying probability model in synthetic datasets. The baseline (LGBM) determines the sample-level optimal policy based on the predictions of a lightGBM model, which is also the teacher model. All experiments were run on an Intel 8-core i7 PC with 32GB RAM. CPLEX 20.1 was used to solve the RMP. The minimum number of samples per rule for SPMT is set to 10. $K = 100$ for KSP.

Synthetic Datasets

We follow the identical setup in Biggs, Sun, and Ettl 2021, where we generate six datasets consisting entirely of numerical features, simulated from different generative demand models. The data generation process can be found in the supplementary materials. We train a gradient boosted tree ensemble model using the lightGBM package (Ke et al. 2017) as the teacher model. The action set consists of 9 prices, ranging from the 10th to the 90th percentile of observed prices in 10% increments.

Varying policy size We explore how the expected revenue changes with the number of policies. We use a SPT of depth k which is grown to its full width to benchmark against a multiway-split tree (SPMT) with $n = 2^k$ rules, where



(a) Revenue with varying tree depth



(b) Revenue with varying training data size

Figure 2: Experiment results on realized outcome for synthetic Dataset (6)

$k = \{1, \dots, 5\}$. The number of training samples is held constant at $M = 5000$. For each tree depth, we run 10 independent simulations for each dataset and each k (i.e., 300 experiments in total). We highlight the results for $k = 3$ and 5 in Table 1, which summarizes mean revenue over the simulations. Fig 2a shows the performance on dataset (6) with respect to the number of rules as an illustrative example, while detailed results for individual datasets are included in the supplementary materials.

Although both SPMT and SPT use the same teacher model, SPMT generally outperforms SPT, which employs a greedy heuristic, as seen in the modest gains shown in the experiments. Furthermore, SPT is unable to incorporate constraints, a shortcoming which severely limits its usefulness.

Varying data size We also investigate how SPMT performs as the size of the samples increases, where $M = \{100, 300, 10^3, 3 \times 10^3, 10^4, 3 \times 10^4, 10^5, 3 \times 10^5, 6 \times 10^5, 9 \times 10^5, 10^6\}$. We focus on $n = 8$ and 32 rules, again for 10 independent iterations for each configuration (i.e., 220 experiments) using Dataset (6). Fig 2b shows the result on realized revenue versus data size M .¹

The baseline LGBM is an upper bound to SPMT in theory since the latter trades off performance for interpretability. It can be seen as the revenue gap between LGBM and SPMT policies Fig 2b when the training sample size becomes large and the lgbm model produces a more accurate estimate of the underlying groundtruth. With small sample sizes, LGBM may overfit and the realized outcome may appear worse/noisier. It is crucial to note that policy from the LGBM baseline is not interpretable and can be potentially very complex (such as a fully personalized price). It is also not surprising that a policy with more rules generally outperforms fewer rules. However, once the sample size exceeds 3×10^4 , both policies with $n = 8$ and 32 converge to the same realized revenue and we do not observe further improvement from either policy by increasing the sample size.

Runtime study We investigate CG runtime as the sample size M increases from 100 to 10^6 , with the same setup de-

scribed earlier. In our experiments, all RMP instances converged in less than 20 CG iterations, with 11.19 (1.33) seconds for each iteration of RMP and KSP. Detailed results are available in the supplementary material. The key observation is that our proposed SPMT approach is inherently more scalable than prior MIP approaches when near-optimal solutions suffice. In the experiment which allowed up to 32 rules for the dataset having 10^6 samples, prior MIP models would require more than 32×10^6 binary variables. In comparison, our Master-MIP required less than 3000 binary variables.

Real Datasets

Grocery pricing case study We consider the problem of grocery pricing, using a publicly available dataset² that contains over two years of household level transactions from a group of 2,500 households at a grocery retailer. A processed dataset with 97,295 rows which contain both purchases and “no-purchases” of strawberries is available online.³

The unconstrained use case of maximizing expected revenue has been studied in Biggs, Sun, and Ettl 2021 and Amram, Dunn, and Zhuo 2020. We follow the same experiment setup described in these papers, where we divide the data in halves, and independently train a teacher and an evaluator (as the ground truth) using lightGBM. With $n = 64$, SPMT policy achieves 82.8% increase in revenue over the historical baseline, compared to 65.9% and 77.1% reported in Biggs, Sun, and Ettl 2021 and Amram, Dunn, and Zhuo 2020 respectively. Noting that the latter work and our approach both seek optimal prescriptive policies, the difference in gain highlights the benefit of a multiway-split tree over a binary-split tree, for being more informative. An example of a SPMT with $n = 8$ is shown in Fig 1b.

There are two drawbacks with the existing unconstrained policy. First, its predicted demand almost doubles the historical sales, which may not be realizable due to supply constraints and other limitations. Second, the price discrimination based on customer-level features raises legal and fairness concerns. We briefly describe two constrained scenar-

¹We omitted SPT here because its current implementation from Biggs, Sun, and Ettl 2021 is struggling with datasets larger than 30K samples. See supplementary material for more discussions.

²<https://www.dunnhumby.com/careers/engineering/sourcefiles>

³https://docs.interpretable.ai/stable/examples/grocery_pricing/

Dataset	optimal	lgbm	n = 8 / k = 3		n = 32 / k = 5	
			SPMT	SPT	SPMT	SPT
1	3.275 (0.016)	3.161 (0.054)	3.233 (0.038)	3.201 (0.071)	3.201 (0.053)	3.188 (0.063)
2	2.963 (0.034)	2.716 (0.038)	2.166 (0.034)	2.127 (0.042)	2.378 (0.015)	2.277 (0.039)
3	3.420(0.006)	3.275 (0.064)	3.347(0.048)	3.331(0.052)	3.336(0.047)	3.333(0.047)
4	3.492(0.012)	3.344 (0.057)	3.365(0.051)	3.343(0.079)	3.379(0.055)	3.366(0.06)
5	3.35(0.007)	3.260 (0.029)	3.291(0.056)	3.260(0.067)	3.296(0.017)	3.287(0.022)
6	2.592(0.01)	2.456 (0.033)	2.459(0.033)	2.429(0.064)	2.464(0.016)	2.447(0.029)

Table 1: Comparison on realized outcome for synthetic datasets ($M = 5000$)

ios to address these issues, where more details are provided in the supplementary material. First, stores are grouped into 5 clusters based on historical sales and we require the predicted demand under a new pricing policy does not deviate too much from the historical average. With $n = 64$, SPMT produces rules that result in 47.49% and 61.72% increase in revenue when the allowable change in predicted demand is set to 25% and 50% of the historical value. In a separate scenario, we use inter-rule constraints to model a store-based loyalty pricing policy, where all shoppers at a store receive the same price except loyalty-card shoppers, who receive a price that is same or lower. This setting is an example of inter-rule constraints involving logical conjunctions of categorical and numerical features (StoreID, Loyalty, Price), which are handled naturally in our path-based MIP, but relatively difficult to express efficiently using arc-based feature-level models. The resulting pricing policy using only storeID and a loyalty indicator to define rules achieves 65.4% increase in revenue over the baseline without discriminating customers based on their personal features.

Housing upgrade use case We consider a Kaggle dataset on house prices⁴ that includes numerical and categorical attributes such as age, square footage, number of bedrooms, bathrooms, zipcode, as well as grade, i.e., an index from 1-13, where higher value indicates better construction and design. We first train a regression model to predict the house value given the attributes as the teacher. We then formulate a prescriptive problem, i.e., maximize the predicted sale price in the test set by adjusting the grade of individual houses. As the teacher model predicts that grade increases the house value, an unconstrained policy search simply recommends that all houses upgrade to the highest level.

One of the constrained scenarios that we consider requires houses to “conform to the neighborhood”, i.e., the predicted sale price of houses with the same zip code must be within 10% of the historical value. The decision rules no longer upgrade all houses but prescribe a mix of upgrades and downgrades based on other housing features while satisfying the price constraint for each neighborhood. More constrained scenarios are included in the supplementary materials.

Airline pricing use case We consider the task of pricing premium seats for a large airline (an industry partner) using easily interpretable prescriptive rules. The dataset contains more than 1.3 million samples across multiple markets

with several features such as departure day and time, duration of the flight, market, whether one-way or round trip. We want to point out that our work allows multiple actions to be added as stacks of action nodes e.g., to represent the prices for the first class, business class and premium economy seats respectively. Structured decision making can be modeled as constraints, e.g., given the same trip information, a business class (premium economy) seat should be at least \$250 cheaper than a first (business) class seat. For confidentiality reasons, details of the study are omitted.

We compare the policies from the greedy SPT and our proposed SPMT method for a same number of decision rules. With SPT, seat capacity limits were violated and resulted in a overly high predicted gain. Further analysis revealed that these rules would have allowed early bookers to purchase premium seats at a bargain, cannibalizing the demand from high-value customers who typically show up later. By adding market-specific capacity constraints on the predicted conversions, we revised the rules to achieve a more realistic gain that is more likely to be realized in live settings.

Conclusion

Our work adds to a stream of growing research which deserves more attention in the literature due to its paramount practical importance, i.e., generating interpretable policy from data for decision making. We address the problem of distilling prescriptive rules using a teacher model, providing counterfactual estimates. We formulate a mixed integer optimization problem to distill active decision rules that are shown to represent a multiway-split tree on an acyclic feature graph. The number of binary decision variables in our model can increase exponentially in the number of features that comprise the rules. As only a small subset of rules are active in an optimal solution, we propose a column generation approach to solve the MIP. Our method can handle complex inter-rule and intra-rule constraints that cannot be satisfied by existing prescriptive tree methods. We provide computational results on synthetic and publicly available real-life data and solve instances having up to a million samples within an hour of computation time. The proposed method offers a generic and widely applicable way of generating (near) optimal prescriptive rules by transforming blackbox AI/ML predictions into operationally effective decisions that may benefit enterprises.

⁴<https://www.kaggle.com/harlfoxem/housesalesprediction>

References

- Aghaei, S.; Azizi, M. J.; and Vayanos, P. 2019. Learning optimal and fair decision trees for non-discriminative decision-making. In *Proceedings of the AAAI Conference on Artificial Intelligence*, volume 33, 1418–1426.
- Aghaei, S.; Gomez, A.; and Vayanos, P. 2020. Learning optimal classification trees: Strong max-flow formulations. *arXiv preprint arXiv:2002.09142*.
- Amram, M.; Dunn, J.; and Zhuo, Y. D. 2020. Optimal Policy Trees. *arXiv preprint arXiv:2012.02279*.
- Atamtürk, A.; Nemhauser, G. L.; and Savelsbergh, M. W. 1996. A combined Lagrangian, linear programming, and implication heuristic for large-scale set partitioning problems. *Journal of heuristics*, 1(2): 247–259.
- Athey, S.; and Imbens, G. 2016. Recursive partitioning for heterogeneous causal effects. *Proceedings of the National Academy of Sciences*, 113(27): 7353–7360.
- Bach, F. 2008. Exploring large feature spaces with hierarchical multiple kernel learning. *arXiv preprint arXiv:0809.1493*.
- Barnhart, C.; Johnson, E. L.; Nemhauser, G. L.; Savelsbergh, M. W.; and Vance, P. H. 1998. Branch-and-price: Column generation for solving huge integer programs. *Operations research*, 46(3): 316–329.
- Bertsimas, D.; and Dunn, J. 2017. Optimal classification trees. *Machine Learning*, 106(7): 1039–1082.
- Bertsimas, D.; Dunn, J.; and Mundru, N. 2019. Optimal prescriptive trees. *INFORMS Journal on Optimization*, 1(2): 164–183.
- Biggs, M.; Sun, W.; and Ettl, M. 2021. Model Distillation for Revenue Optimization: Interpretable Personalized Pricing. In *International Conference on Machine Learning*, 946–956. PMLR.
- Breiman, L.; Friedman, J.; Stone, C. J.; and Olshen, R. A. 1984. *Classification and regression trees*. CRC press.
- Bront, J. J. M.; Méndez-Díaz, I.; and Vulcano, G. 2009. A column generation algorithm for choice-based network revenue management. *Operations research*, 57(3): 769–784.
- Carvalho, D. V.; Pereira, E. M.; and Cardoso, J. S. 2019. Machine learning interpretability: A survey on methods and metrics. *Electronics*, 8(8): 832.
- Chen, Z.-L.; and Xu, H. 2006. Dynamic column generation for dynamic vehicle routing with time windows. *Transportation Science*, 40(1): 74–88.
- CPLEX, I. 2020. Introducing IBM ILOG CPLEX Optimization Studio 20.1.0. <https://www.ibm.com/docs/en/icos/20.1.0>. Accessed: 2021-03-25.
- Desaulniers, G.; Desrosiers, J.; and Solomon, M. M. 2006. *Column generation*, volume 5. Springer Science & Business Media.
- Dudík, M.; Langford, J.; and Li, L. 2011. Doubly Robust Policy Evaluation and Learning. In *ICML*.
- Ford Jr, L. R.; and Fulkerson, D. R. 1958. A suggested computation for maximal multi-commodity network flows. *Management Science*, 5(1): 97–101.
- Frosst, N.; and Hinton, G. 2017. Distilling a neural network into a soft decision tree. *arXiv preprint arXiv:1711.09784*.
- Fulton, T.; Kasif, S.; and Salzberg, S. 1995. Efficient algorithms for finding multi-way splits for decision trees. In *Machine Learning Proceedings 1995*, 244–251. Elsevier.
- Fürnkranz, J. 2017. *Decision Lists and Decision Trees*, 328–329.
- Guidotti, R.; Monreale, A.; Ruggieri, S.; Turini, F.; Giannotti, F.; and Pedreschi, D. 2018. A survey of methods for explaining black box models. *ACM computing surveys (CSUR)*, 51(5): 1–42.
- Hinton, G.; Vinyals, O.; and Dean, J. 2015. Distilling the knowledge in a neural network. *arXiv preprint arXiv:1503.02531*.
- Hirano, K.; and Imbens, G. W. 2004. The propensity score with continuous treatments. *Applied Bayesian modeling and causal inference from incomplete-data perspectives*, 226164: 73–84.
- Horne, G. 1980. Finding the K least cost paths in an acyclic activity network. *Journal of the Operational Research Society*, 31(5): 443–448.
- Irnich, S.; and Desaulniers, G. 2005. Shortest path problems with resource constraints. In *Column generation*, 33–65. Springer.
- Jawanpuria, P.; Nath, J. S.; and Ramakrishnan, G. 2011. Efficient rule ensemble learning using hierarchical kernels. In *ICML*.
- Kallus, N. 2017. Recursive partitioning for personalization using observational data. In *Proceedings of the 34th International Conference on Machine Learning-Volume 70*, 1789–1798. JMLR. org.
- Ke, G.; Meng, Q.; Finley, T.; Wang, T.; Chen, W.; Ma, W.; Ye, Q.; and Liu, T.-Y. 2017. Lightgbm: A highly efficient gradient boosting decision tree. In *Advances in neural information processing systems*, 3146–3154.
- Klabjan, D.; Johnson, E. L.; Nemhauser, G. L.; Gelman, E.; and Ramaswamy, S. 2002. Airline crew scheduling with time windows and plane-count constraints. *Transportation science*, 36(3): 337–348.
- Künzel, S. R.; Sekhon, J. S.; Bickel, P. J.; and Yu, B. 2019. Metalearners for estimating heterogeneous treatment effects using machine learning. *Proceedings of the national academy of sciences*, 116(10): 4156–4165.
- Laurent, H.; and Rivest, R. L. 1976. Constructing optimal binary decision trees is NP-complete. *Information processing letters*, 5(1): 15–17.
- Lepeniotti, K.; Bousdekis, A.; Apostolou, D.; and Mentzas, G. 2020. Prescriptive analytics: Literature review and research challenges. *International Journal of Information Management*, 50: 57–70.
- Liu, G.; Schulte, O.; Zhu, W.; and Li, Q. 2018. Toward interpretable deep reinforcement learning with linear model utrees. In *Joint European Conference on Machine Learning and Knowledge Discovery in Databases*, 414–429. Springer.

Lundberg, S. M.; and Lee, S.-I. 2017. A unified approach to interpreting model predictions. In *Advances in neural information processing systems*, 4765–4774.

Miller, T. 2019. Explanation in artificial intelligence: Insights from the social sciences. *Artificial intelligence*, 267: 1–38.

Puiutta, E.; and Veith, E. M. 2020. Explainable reinforcement learning: A survey. In *International Cross-Domain Conference for Machine Learning and Knowledge Extraction*, 77–95. Springer.

Ribeiro, M. T.; Singh, S.; and Guestrin, C. 2016. ”Why should I trust you?” Explaining the predictions of any classifier. In *Proceedings of the 22nd ACM SIGKDD international conference on knowledge discovery and data mining*, 1135–1144.

Shalit, U.; Johansson, F. D.; and Sontag, D. 2017. Estimating individual treatment effect: generalization bounds and algorithms. In *International Conference on Machine Learning*, 3076–3085. PMLR.

Subramanian, S.; and Sherali, H. D. 2008. An effective deflected subgradient optimization scheme for implementing column generation for large-scale airline crew scheduling problems. *INFORMS Journal on Computing*, 20(4): 565–578.

Wager, S.; and Athey, S. 2018. Estimation and inference of heterogeneous treatment effects using random forests. *Journal of the American Statistical Association*, 113(523): 1228–1242.

Wolsey, L. A.; and Nemhauser, G. L. 1999. *Integer and combinatorial optimization*, volume 55. John Wiley & Sons.

Xu, Y. 2019. Solving Large Scale Optimization Problems in the Transportation Industry and Beyond Through Column Generation. In *Optimization in Large Scale Problems*, 269–292. Springer.

Zhou, Z.; Athey, S.; and Wager, S. 2018. Offline multi-action policy learning: Generalization and optimization. *arXiv preprint arXiv:1810.04778*.

Zhu, H.; Murali, P.; Phan, D.; Nguyen, L.; and Kalagnanam, J. 2020. A Scalable MIP-based Method for Learning Optimal Multivariate Decision Trees. In *Advances in Neural Information Processing Systems*, volume 33, 1771–1781.

References

Aghaei, S.; Azizi, M. J.; and Vayanos, P. 2019. Learning optimal and fair decision trees for non-discriminative decision-making. In *Proceedings of the AAAI Conference on Artificial Intelligence*, volume 33, 1418–1426.

Aghaei, S.; Gomez, A.; and Vayanos, P. 2020. Learning optimal classification trees: Strong max-flow formulations. *arXiv preprint arXiv:2002.09142*.

Amram, M.; Dunn, J.; and Zhuo, Y. D. 2020. Optimal Policy Trees. *arXiv preprint arXiv:2012.02279*.

Atamtürk, A.; Nemhauser, G. L.; and Savelsbergh, M. W. 1996. A combined Lagrangian, linear programming, and implication heuristic for large-scale set partitioning problems. *Journal of heuristics*, 1(2): 247–259.

Athey, S.; and Imbens, G. 2016. Recursive partitioning for heterogeneous causal effects. *Proceedings of the National Academy of Sciences*, 113(27): 7353–7360.

Bach, F. 2008. Exploring large feature spaces with hierarchical multiple kernel learning. *arXiv preprint arXiv:0809.1493*.

Barnhart, C.; Johnson, E. L.; Nemhauser, G. L.; Savelsbergh, M. W.; and Vance, P. H. 1998. Branch-and-price: Column generation for solving huge integer programs. *Operations research*, 46(3): 316–329.

Bertsimas, D.; and Dunn, J. 2017. Optimal classification trees. *Machine Learning*, 106(7): 1039–1082.

Bertsimas, D.; Dunn, J.; and Mundru, N. 2019. Optimal prescriptive trees. *INFORMS Journal on Optimization*, 1(2): 164–183.

Biggs, M.; Sun, W.; and Ettl, M. 2021. Model Distillation for Revenue Optimization: Interpretable Personalized Pricing. In *International Conference on Machine Learning*, 946–956. PMLR.

Breiman, L.; Friedman, J.; Stone, C. J.; and Olshen, R. A. 1984. *Classification and regression trees*. CRC press.

Bront, J. J. M.; Méndez-Díaz, I.; and Vulcano, G. 2009. A column generation algorithm for choice-based network revenue management. *Operations research*, 57(3): 769–784.

Carvalho, D. V.; Pereira, E. M.; and Cardoso, J. S. 2019. Machine learning interpretability: A survey on methods and metrics. *Electronics*, 8(8): 832.

Chen, Z.-L.; and Xu, H. 2006. Dynamic column generation for dynamic vehicle routing with time windows. *Transportation Science*, 40(1): 74–88.

CPLEX, I. 2020. Introducing IBM ILOG CPLEX Optimization Studio 20.1.0. <https://www.ibm.com/docs/en/icos/20.1.0>. Accessed: 2021-03-25.

Desaulniers, G.; Desrosiers, J.; and Solomon, M. M. 2006. *Column generation*, volume 5. Springer Science & Business Media.

Dudík, M.; Langford, J.; and Li, L. 2011. Doubly Robust Policy Evaluation and Learning. In *ICML*.

Ford Jr, L. R.; and Fulkerson, D. R. 1958. A suggested computation for maximal multi-commodity network flows. *Management Science*, 5(1): 97–101.

Frosst, N.; and Hinton, G. 2017. Distilling a neural network into a soft decision tree. *arXiv preprint arXiv:1711.09784*.

Fulton, T.; Kasif, S.; and Salzberg, S. 1995. Efficient algorithms for finding multi-way splits for decision trees. In *Machine Learning Proceedings 1995*, 244–251. Elsevier.

Fürnkranz, J. 2017. *Decision Lists and Decision Trees*, 328–329.

Guidotti, R.; Monreale, A.; Ruggieri, S.; Turini, F.; Giannotti, F.; and Pedreschi, D. 2018. A survey of methods for explaining black box models. *ACM computing surveys (CSUR)*, 51(5): 1–42.

Hinton, G.; Vinyals, O.; and Dean, J. 2015. Distilling the knowledge in a neural network. *arXiv preprint arXiv:1503.02531*.

- Hirano, K.; and Imbens, G. W. 2004. The propensity score with continuous treatments. *Applied Bayesian modeling and causal inference from incomplete-data perspectives*, 226164: 73–84.
- Horne, G. 1980. Finding the K least cost paths in an acyclic activity network. *Journal of the Operational Research Society*, 31(5): 443–448.
- Irnich, S.; and Desaulniers, G. 2005. Shortest path problems with resource constraints. In *Column generation*, 33–65. Springer.
- Jawanpuria, P.; Nath, J. S.; and Ramakrishnan, G. 2011. Efficient rule ensemble learning using hierarchical kernels. In *ICML*.
- Kallus, N. 2017. Recursive partitioning for personalization using observational data. In *Proceedings of the 34th International Conference on Machine Learning-Volume 70*, 1789–1798. JMLR. org.
- Ke, G.; Meng, Q.; Finley, T.; Wang, T.; Chen, W.; Ma, W.; Ye, Q.; and Liu, T.-Y. 2017. Lightgbm: A highly efficient gradient boosting decision tree. In *Advances in neural information processing systems*, 3146–3154.
- Klabjan, D.; Johnson, E. L.; Nemhauser, G. L.; Gelman, E.; and Ramaswamy, S. 2002. Airline crew scheduling with time windows and plane-count constraints. *Transportation science*, 36(3): 337–348.
- Künzel, S. R.; Sekhon, J. S.; Bickel, P. J.; and Yu, B. 2019. Metalearners for estimating heterogeneous treatment effects using machine learning. *Proceedings of the national academy of sciences*, 116(10): 4156–4165.
- Laurent, H.; and Rivest, R. L. 1976. Constructing optimal binary decision trees is NP-complete. *Information processing letters*, 5(1): 15–17.
- Lepenioti, K.; Bousdekis, A.; Apostolou, D.; and Mentzas, G. 2020. Prescriptive analytics: Literature review and research challenges. *International Journal of Information Management*, 50: 57–70.
- Liu, G.; Schulte, O.; Zhu, W.; and Li, Q. 2018. Toward interpretable deep reinforcement learning with linear model u-trees. In *Joint European Conference on Machine Learning and Knowledge Discovery in Databases*, 414–429. Springer.
- Lundberg, S. M.; and Lee, S.-I. 2017. A unified approach to interpreting model predictions. In *Advances in neural information processing systems*, 4765–4774.
- Miller, T. 2019. Explanation in artificial intelligence: Insights from the social sciences. *Artificial intelligence*, 267: 1–38.
- Puiutta, E.; and Veith, E. M. 2020. Explainable reinforcement learning: A survey. In *International Cross-Domain Conference for Machine Learning and Knowledge Extraction*, 77–95. Springer.
- Ribeiro, M. T.; Singh, S.; and Guestrin, C. 2016. ” Why should i trust you?” Explaining the predictions of any classifier. In *Proceedings of the 22nd ACM SIGKDD international conference on knowledge discovery and data mining*, 1135–1144.
- Shalit, U.; Johansson, F. D.; and Sontag, D. 2017. Estimating individual treatment effect: generalization bounds and algorithms. In *International Conference on Machine Learning*, 3076–3085. PMLR.
- Subramanian, S.; and Sherali, H. D. 2008. An effective deflected subgradient optimization scheme for implementing column generation for large-scale airline crew scheduling problems. *INFORMS Journal on Computing*, 20(4): 565–578.
- Wager, S.; and Athey, S. 2018. Estimation and inference of heterogeneous treatment effects using random forests. *Journal of the American Statistical Association*, 113(523): 1228–1242.
- Wolsey, L. A.; and Nemhauser, G. L. 1999. *Integer and combinatorial optimization*, volume 55. John Wiley & Sons.
- Xu, Y. 2019. Solving Large Scale Optimization Problems in the Transportation Industry and Beyond Through Column Generation. In *Optimization in Large Scale Problems*, 269–292. Springer.
- Zhou, Z.; Athey, S.; and Wager, S. 2018. Offline multi-action policy learning: Generalization and optimization. *arXiv preprint arXiv:1810.04778*.
- Zhu, H.; Murali, P.; Phan, D.; Nguyen, L.; and Kalagnanam, J. 2020. A Scalable MIP-based Method for Learning Optimal Multivariate Decision Trees. In *Advances in Neural Information Processing Systems*, volume 33, 1771–1781.

Constrained Prescriptive Trees via Column Generation

Supplementary Material

Section 3 - Problem Formulation

Proof of Proposition 1

In the acyclic multi-level directed graph which we consider, $G(V, E)$, each feature indicates a level in the graph, represented by multiple nodes corresponding to its distinct feature values. For each feature, with the exception of the action nodes π , we introduce a dummy node *SKIP*. Without the loss of generality, with a d -dimensional input vector x , action feature π is the last feature (see Fig 1a as an illustrative example). Denote L_f as the number of unique feature values for the f -th feature.

The total number of nodes in G is given by $|V| = \sum_{f=1}^{d-1} (L_f + 1) + L_d + 2$, including the source and sink nodes, i.e., $|V| = O\left(\sum_{f=1}^d L_f\right) = O(d)$. On the other hand, the number of paths from the source to the sink is given by $|\mathcal{P}| = O\left(\prod_{f=1}^d L_f\right) = O(L^d)$, for some constant L .

Proof of Theorem 1

By including *SKIP* nodes, the path set \mathcal{P} which corresponds to the decision rule set includes every possible combination of features. Moreover, the set coverage constraint (3) in SPP has ensured that rules are non-overlapping, i.e., each sample can only be assigned to a single rule. Then we reach the desired result.

Remarks on numerical features

For tree-based approaches, numerical input are typically discretized. For example, consider a numerical feature with values in $[0, 1]$ discretized into $\kappa = 3$ levels, corresponding to 3 intervals $[0, 0.33)$, $[0.33, 0.67)$ and $[0.67, 1.0]$. A naive approach is to create 3 nodes in a multiway-split tree. However, this approach is limiting, considering a binary-split tree can branch on conditions such as $x \leq 0.67$ or $x > 0.3$. We consider a *cumulative binning* method, where intervals can be overlapping. More specifically, we create additional nodes $[0, 0.67)$, $[0, 1.0]$, $[0.33, 1.0]$, yielding a total of 6 nodes. Note that the MIP formulation includes a coverage constraint to ensure that the final rules do not contain overlapping samples. More generally, this binning method results in $O(\kappa^2)$ nodes, i.e, an

improvement in the expressiveness of a rule at the expense of higher computational complexity. More efficient methods to handle numerical features can be employed as a topic for future work.

A similar cumulative binning approach can be adopted to manage categorical features if we want to create nodes associated with multiple levels of a feature. Doing so can improve solution quality at the expense of increased rule complexity.

Section 4 - An Efficient and Scalable Algorithm

Dual formulation of RMP

For the *restricted master problem* (RMP), we 1) consider only a subset of paths, \hat{N} , where \hat{N} is typically much smaller than N , and 2) relax the integrality constraints on z_j to $0 \leq z_j \leq 1$ for all $j = 1, \dots, \hat{N}$. Denote the dual variables associated with the set partitioning constraints in (3) and the cardinality constraint in (4) as λ_i and μ respectively. The dual of the RMP can be written as the following,

$$\begin{aligned}
 \text{(Dual of RMP)} \quad & \max \quad \sum_{i=1}^M \lambda_i + n\mu \\
 & \text{s.t.} \quad \sum_{i=1}^M a_{ij} \lambda_i + \mu \geq r_j, \quad \forall j = 1, \dots, \hat{N} \\
 & \quad \lambda_i \geq -c_i, \forall i = 1, \dots, M \\
 & \quad \mu \geq 0
 \end{aligned}$$

Note that since $z_j \leq 1$ is implied by Eq (3), we are only left with $z_j \geq 0$ in the primal RMP problem.

Remark: A feasible solution to RMP is to set all the slack variables s_i to 0 and add a column that prescribes a single rule for all data samples. The corresponding path in the feature graph passes (only) through all SKIP nodes and then through any of the action nodes.

Section 5 - Experiments

Synthetic datasets

Data generation

We follow the identical setup in Biggs et al. [2021], where six datasets consisting entirely of numerical features are simulated from different generative demand models. For completeness, we include the data generation process below.

The datasets we examine come from the following generative model:

$$Y^* = g(X) + h(X)P + \epsilon, \quad Y = \begin{cases} 1, & \text{if } Y^* > 0 \\ 0, & \text{if } Y^* \leq 0 \end{cases} \quad (1)$$

- Dataset 1: linear probit model with no confounding: $g(X) = X_0$, $h(X) = -1$ and $X \sim N(5, I_2)$ and $P \sim N(5, 1)$.
- Dataset 2: higher dimension probit model with sparse linear interaction $g(X) = 5$, $h(X) = -1.5(X'\beta)$, $\{X_i\}_{i=1}^{20}$, $\{\beta_i\}_{i=1}^5$, $\epsilon_i \sim N(0, 1)$, $P_i \sim N(0, 2)$, $\{\beta_i\}_{i=6}^{20} = 0$, where the purchase probability is only dependent on the first 5 features.
- Dataset 3: probit model with step interaction: $g(X) = 5$, $h(X) = -1.2\mathbb{1}\{X_0 < -1\} - 1.1\mathbb{1}\{-1 \leq X_0 < 0\} - 0.9\mathbb{1}\{0 \leq X_0 < 1\} - 0.8\mathbb{1}\{1 \leq X_0\}$.
- Dataset 4: probit model with multi-dimensional step interaction: $g(X) = 5$, $h(X) = -1.25\mathbb{1}\{X_0 < -1\} - 1.1\mathbb{1}\{-1 \leq X_0 < 0\} - 0.9\mathbb{1}\{0 \leq X_0 < 1\} - 0.75\mathbb{1}\{1 \leq X_0\} - 0.1\mathbb{1}\{X_1 < 0\} + 0.1\mathbb{1}\{X_1 \geq 0\}$.
- Dataset 5: linear probit model with confounding: $g(X) = X_0$, $h(X) = -1$, $X \sim N(5, I_2)$.
- Dataset 6: probit model with non-linear interaction: $g(X) = 4|X_0 + X_1|$, $h(X) = -|X_0 + X_1|$.

We set $X = (X_0, X_1) \sim N(0, I_2)$, $P \sim N(X_0 + 5, 2)$, $\epsilon \sim N(0, 1)$, i.i.d. unless otherwise mentioned. Dataset (1) and (5) are a common demand model used in the pricing literature, with and without confounding effects. Datasets (2)-(4) and (6), have heterogeneity in treatment effects making them suitable for testing personalized pricing. All datasets except dataset (1) and (2) have confounding of observed features, where the price observed is dependent on the features of the item. For the teacher model, we train a gradient boosted tree ensemble model using the lightGBM package Ke et al. [2017]. We use default parameter values, with 50 boosting rounds. The discretized price set is set to 9 prices, ranging from the 10th to the 90th percentile of observed prices in 10% increments.

Additional experiment results

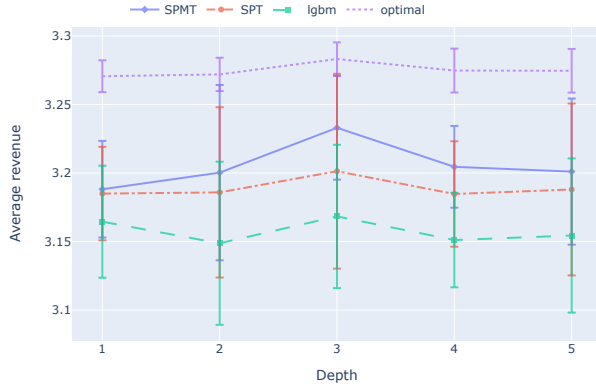
Varying policy size and data size

Figure 1 shows for each of the six datasets, how the expected revenue changes with respect to the depth of the SPT k , or equivalently the rule cardinality in SPMT where $n = 2^k$, for the baselines we benchmark against.

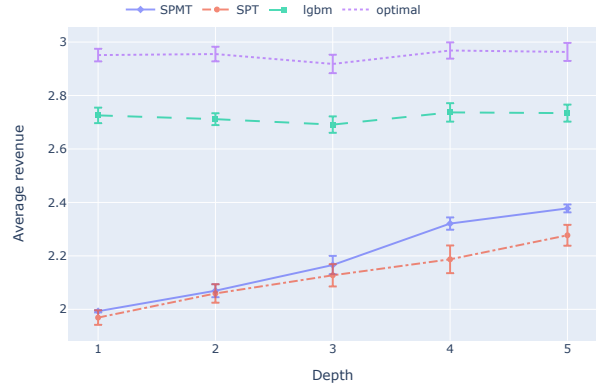
Note that SPT is not shown in Fig 2b) in the main paper, as the code used to produce SPT (courtesy of the authors, Biggs et al. [2021]) was struggling to handle datasets larger than 10K samples and taking several hours to run for each iteration. As a result, we skip this baseline for the experiment in Fig 3b) where we vary sample sizes to 10^6 .

Run time study

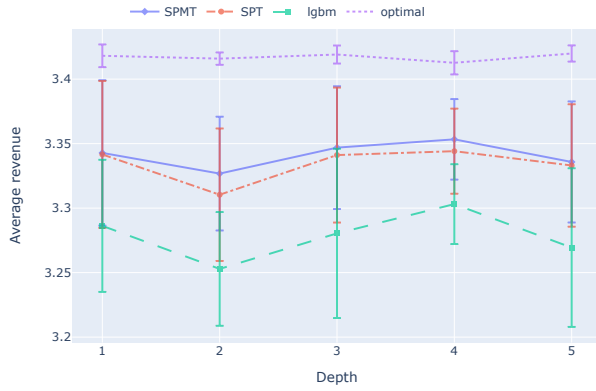
We investigate column generation (CG) runtime as the sample size M increases, where $M = \{100, 300, 10^3, 3 \times 10^3, 10^4, 3 \times 10^4, 10^5, 3 \times 10^5, 6 \times 10^5, 9 \times 10^5, 10^6\}$. We focus on $n = 8$ and 32 rules, again for 10 independent iterations for each configuration (i.e., 220 experiments) using Dataset (6).



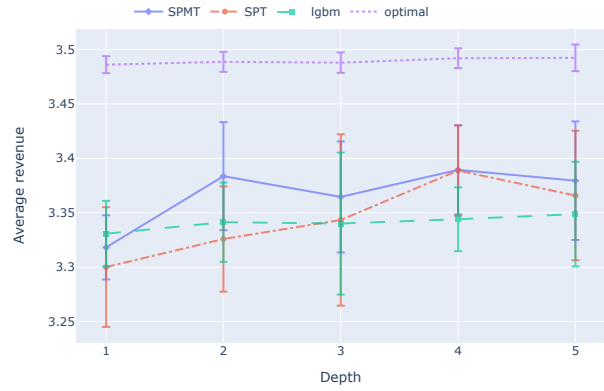
(a) Dataset 1



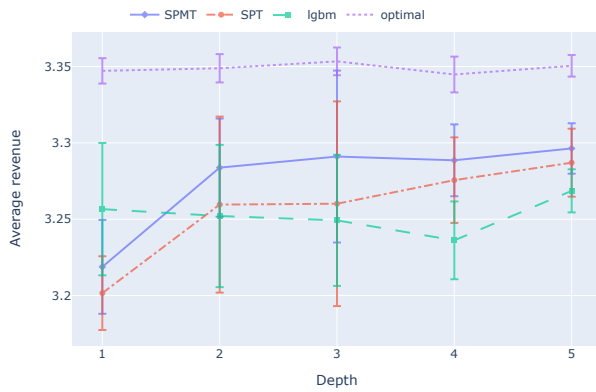
(b) Dataset 2



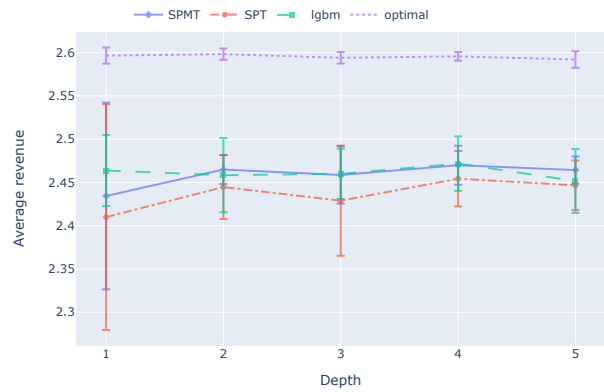
(c) Dataset 3



(d) Dataset 4



(e) Dataset 5



(f) Dataset 6

Figure 1: Experiments synthetic data with increasing tree depth k of SPT, equivalently rule complexity $n = 2^k$ in SPMT

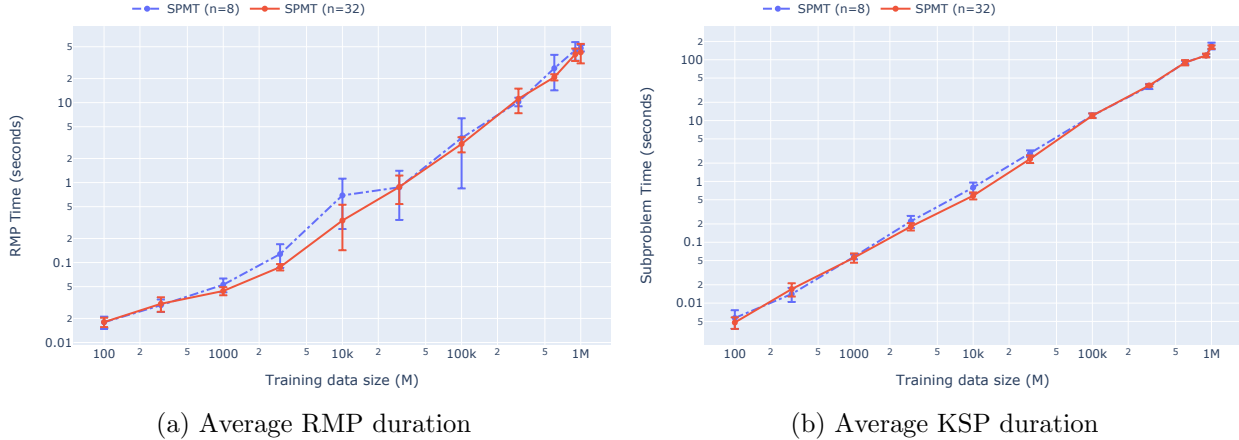


Figure 2: Runtime results for synthetic Dataset (6)

The run time per iteration of CG equals the sum of the RMP and KSP run times. The RMP, being a linear program can be solved in polynomial time (Bazaraa et al. [2008]). The KSP is solved using a naive implementation of a K -shortest path search on an acyclic graph and is bounded by $O(K|V|^2M \log M)$. The first term ($K|V|^2$) represents the worst case run time for a K -shortest path algorithm on an acyclic graph (Horne [1980]), and the $(M \log M)$ term captures the time required to update the training samples (sort and store as trees) covered by the path after every partial path extension. More efficient implementations can be employed to reduce the KSP run time.

The log-log plots in Fig 2 show the average time taken to solve RMP and KSP, normalized by the number of CG iterations taken to converge. These metrics represent the computational effort required per CG iteration, independent of the data-dependent “difficulty” of the problem, which determines whether fewer or more CG iterations are required to converge. In our experiments, all instances took less than 20 CG iterations to converge, with 11.19 and 1.33 seconds as the mean and standard deviation.

We do not observe significant change in these two metrics when we increase the cardinality of the rule set n . In fact, allowing more rules tends to reduce the runtime, as less work is required to “finetune” the rule set. As the samples increase, we observe a super-linear rise in the runtime per CG iteration that approximately follows a $M \log M$ trend. The average KSP runtime for the million sample data set was about 166 seconds while the RMPs were usually solved within 45 seconds by the CPLEX Barrier solver, enabling the CG algorithm to converge to a near optimal solution in about an hour.

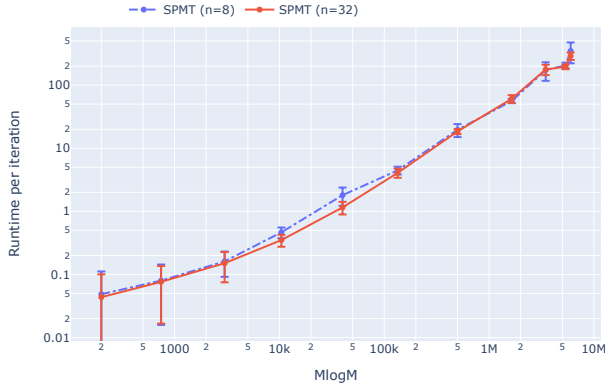
Figure 3 provides additional information on the runtime experiments on Dataset (6). More specifically, total runtime records the amount of time (in seconds) to solve an instance, i.e., I/O operations, column generation (CG) iterations until convergence (including time taken to solve RMP and the subproblem), and the final Master-MIP to obtain an integral solution. Average runtime is the total runtime divided by the number of CG iterations. Note that optimizing the model exactly is an NP-Hard problem, which can be time-consuming for large, challenging problem instances. For simplicity and replicability, we solve our final Master-MIP directly using a standard optimization library (CPLEX, 2020) to distill a (near) optimal subset of prescriptive decision rules.



(a) Total runtime



(b) Average runtime per CG iteration



(c) Average runtime against $M \log M$

Figure 3: Runtime experiment for Dataset (6)

The key takeaway from the runtime study is that our SPMT approach is more scalable in practical settings than prior MIP approaches such as Bertsimas et al. [2019], Amram et al. [2020], since the latter’s MIP model requires $O(2^k M)$ binary variables. For example, in the experiment which allowed a maximum of 32 rules for a dataset with 10^6 training samples, prior MIP models would require more than 32×10^6 binary variables to be added upfront to obtain any answer. In comparison, the Master-MIP in SPMT required less than 3000 binary variables to obtain near-optimal solutions.

To demonstrate the efficacy of column generation in finding high quality solutions for large instances that have several million possible rules, we analyzed ten random instances of Dataset (2) containing 10^6 data samples each for the multiway-split tree with $n = 8$ and 32 respectively. Dataset (2) was chosen for this study because of its relatively larger feature space. Prior to constructing the tree, we analyzed the feature importance of the teacher model using SHAP package (Lundberg and Lee,

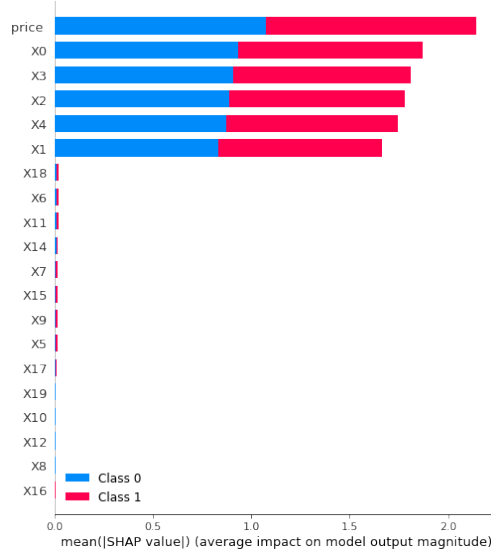


Figure 4: Feature importance based on the teacher model trained on Dataset (2)

2017), which correctly identifies five features along with price as the most predictive features on the outcome, which are used to construct the feature graph (see Fig 4). This highlights a benefit of decoupling prediction from the downstream policy optimization task, as the prescriptive student is able to utilize the teacher’s knowledge to efficiently filter out the uninformative features and construct a more compact feature graph.

Each of the five numerical features were discretized into 12 bins ($\kappa = 4$) using the cumulative binning method discussed earlier. The number of possible paths for this setting in combination with 9 price levels is $13^5 \times 9$, which results in more than 3.3 million possible rules. We compare the relative gap between between the RMP objective function and the teacher model predicted outcome (obtained by selecting the revenue-maximizing price for each sample). Note that the predicted teacher outcome acts as a global upper bound (UB), which may not be achievable for a fixed n where n is much smaller than M . For this experiment, we set $K = 500$ and a maximum time limit of one hour for the CG iterations to reduce the relative gap between the achieved RMP objective function and the UB to 10%. If the CG does not converge within the time limit, we terminate the column generation and solve the Master-MIP. Meanwhile, no time limit is imposed on solving the resultant Master-MIP. The achieved RMP objective function value after each CG iteration is depicted in Fig 5.

Table 1 reports on the average values of achieved MIP and LP (RMP) objective function values expressed in terms of the percentage gap from UB, followed by the final number of z -variables (RMP columns), and the average run time (in minutes) for solving the RMP, the subproblem and the Master-MIP. The standard deviations over ten instances are shown in parentheses. This table shows that with $n = 32$ rules, the solution is within 10.3% of UB, whereas the average final gap that permits no more than 8 rules is 17%. We observe small differences between this final LP and MIP gaps from UB that is less than 0.17% and 0.61% with $n = 32$ and 8, respectively. Note that it is not necessary to solve the LP to provable optimality in practical settings where exact solutions are

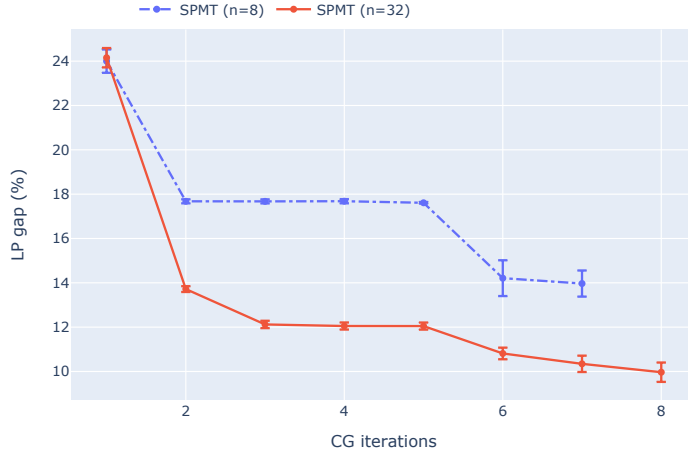


Figure 5: Progression of column generation for Dataset (2)

not required. In this case, the achieved LP objective is not a guaranteed bound on a global optimal solution but is a valid bound on the Restricted Master MIP objective. This narrow MIP-LP gap highlights the benefit of converging to a relatively small pool of high quality rules from which an effective subset of final rules can be recovered via a standard MIP solver.

A key finding in this experiment is that through column generation we required less than 3000 positive reduced cost paths in all instances to distill a near-optimal set with at most 32 rules. This translates to $\hat{N} < 0.0009N$, i.e. an RMP having less than 0.1% of all possible binary variables, which represents a dramatic reduction in the problem’s effective complexity. Even fewer paths (less than 0.05% of all possibilities) were required for $n = 8$ rules. In comparison, for $n = 32$ rules, prior MIP approaches would require a model having more than 30 million binary variables to be formulated, which would be computationally intractable.

In terms of runtime, Table 1 shows that a 10.3% gap from UB was achieved with $n = 32$ in slightly more than an hour. The maximum time limit for CG iterations was reached in all instances for $n = 32$. In contrast, the average run time for $n = 8$ to attain a solution gap of 17% from UB was relatively lower (about 39 minutes) albeit with a higher standard deviation, as the CG iterations converged before the time limit in seven of the ten instances. However, as seen in Fig 5, the achieved LP gap % with $n = 32$ after just two CG iterations is better than the final LP gap achieved with $n = 8$. A less restrictive cardinality constraint resulted in faster convergence to the same solution quality in our experiments.

Real datasets

We perform multiple experiments with real datasets to demonstrate the practical benefits of adding various intra-rule and inter-rule constraints to satisfy critical real-life requirements. Specifically, we are able to identify non-discriminatory and transparent prescriptive policies that also increase

Table 1: Worst-case optimality gap and runtime for Dataset (2)

Rules (n)	MIP gap %	LP gap %	RMP columns	Average runtime (min)
8	17.033 (2.031)	16.581 (1.827)	811 (363)	38.579 (16.972)
32	10.281 (0.457)	10.164 (0.452)	2539 (251)	65.351 (5.155)

revenue, operational effectiveness, and proactively avoid inter-rule conflicts. We achieve this task in two steps. First, we execute the CG algorithm in an “unconstrained” mode, where we do not consider additional restrictions beyond the rule-cardinality constraint. Subsequently, in one or more “constrained” modes, we impose additional side constraints and report on the performance improvements with respect to the different goals.

Grocery pricing case study

One potential issue with the unconstrained pricing policy is its significantly high demand predicted by the teacher model. Compared to the median historical price of \$2.99 for 1 pound of strawberries, the bulk of the optimal policies suggest a large price cut to \$2 as shown in Fig 1b in the main paper. The key insight is that the demand for strawberries is elastic across many segments, i.e., a decrease in price leads to a significant increase in demand and its revenue. In fact, the predicted demand at the optimal prescribed policy is 99.94% higher than the historical value. Such demand surge may be neither realistic nor desirable due to supply constraint or other limits imposed by the perishable nature of the product. Such observations motivate us to investigate this use case by imposing realistic operational constraints.

We derive two features to facilitate store-cluster pricing and loyalty pricing. More specifically, we create a feature called “Cluster” as we group 311 stores in the dataset into 5 clusters, i.e., “extremely low”, “low”, “medium”, “high” and “mega” sales segments, based on their past sales by using the following cutoff: [0, 2, 15, 30, 100, 300]. That is, a store with total sales within [15, 30) will be assigned to “medium” sales cluster. Note that in this dataset, 199 stores fall into the “extremely low” sales cluster. Meanwhile, we also create a binary indicator “Loyalty” to indicate whether the customer is a loyalty card holder. To achieve this, we analyze the original Dunnhumby dataset¹. For each customer, Loyalty = 1 if one of her historical transactions (not restricted to strawberry purchases) contains a non-zero “retail_disc” value which indicates a retail discount applied due to a loyalty card. Based on this definition, in the processed dataset² on strawberry purchases, 465 out of 547 customers are identified as loyalty card holders.

With store-cluster pricing, we impose a constraint for each cluster which requires the predicted demand under a new pricing policy does not deviate too much from the historical average. With 64 rules, SPMT produces policies that result in 47.49% and 61.72% increase in revenue over the historical policy when the allowable change in predicted demand is set to 25% and 50% of the historical value for each cluster. Unsurprisingly, more stringent capacity constraint results in lower revenue.

¹<https://www.dunnhumby.com/careers/engineering/sourcefiles>

²https://docs.interpretable.ai/stable/examples/grocery_pricing/

With loyalty price, we use StoreID and Loyalty indicator as features for the tree, where all shoppers at a store receive the same price except loyalty-card shoppers, who receive a price that is same or lower. After applying these constraints, SPMT recommends a policy which leads to 65.4% improvement in revenue over the historical baseline.

Housing upgrade use case

This use case is different from other studies in the paper because the teacher model addresses a regression problem, i.e., predict the sales price of a house given its attributes, as opposed to being a classifier. We assume that the houses in the evaluation data are yet to be constructed and their grades can be altered to change their predicted sales prices. The predicted gain is given by the sum of the teacher predicted sales prices. Numerical features such as living area and age were aggregated into bins and the CG algorithm was run on the resulting data set. The output decision rules were then evaluated on the properties listed in the test data.

We first analyze the unconstrained setting. The unconstrained policy yields a single decision rule to upgrade to the highest level, which essentially increases the predicted sales prices of all houses to their highest value and results in a 124% gain in the test data. However, such a rule destroys the price diversity of the houses in a neighborhood and ignores that the incremental investment required to upgrade all houses. The other two scenarios address these concerns using constraints.

A key feature of our approach is the ability to manage constraints to ensure fair and operationally effective prescriptive rules. Using a constrained housing scenario as an example, we explain how inter-rule or global constraints are satisfied. Suppose we impose a “zip-4” pricing constraint at the neighborhood level that ensure that the average predicted sales price of houses having the same first 4 digits of the zip code cannot change by more than 10%. There are a total of 19 such localities in the dataset and this restriction is applied to each of them as discussed below.

Such a constraint can be added to the RMP, resulted in a slightly different reduced cost to guide column generation. Denote $d_{il} = 1$ if house i is in zipcode l , 0 otherwise, p_l as the historical sale price for zipcode l . Recall g_{i,q_j} is the predicted counterfactual outcome (sale price) associated with rule j for sample (house) i . The required constraint can be formulated as,

$$0.9p_l \leq \frac{1}{\sum_i d_{il}} \sum_j \sum_i d_{il} g_{i,q_j} z_j \leq 1.1p_l, \quad \forall i, l \tag{A.1}$$

Eq A.1 is simply a linear constraint as d_{il} and g_{i,q_j} are parameters to the optimization problem. We can rewrite Eq A.1 as

$$\frac{1}{\sum_i d_{il}} \sum_j \sum_i d_{il} g_{i,q_j} z_j \leq 1.1p_l,$$

and

$$-\frac{1}{\sum_i d_{il}} \sum_j \sum_i d_{il} g_{i,q_j} z_j \leq -0.9p_l.$$

Let ρ_{l+}^t and ρ_{l-}^t denote the non-negative dual variables associated with these two sets of constraints

respectively. Then the reduced cost can be written as

$$rc_j^t = r_j^t - \left(\sum_i a_{ij} \lambda_i^t + \mu^t + \sum_i \sum_l \frac{1}{\sum_i d_{il}} d_{il} g_{i,q_j} (\rho_{l+}^t - \rho_{l-}^t) \right).$$

More generally, inter-rule constraints which span across several paths/rules (e.g., the cardinality constraint as Eq (4) in the main paper and Eq A.1) enter the RMP formulation. They influence the subproblem through the resultant reduced costs to ensure that paths that are more likely to be feasible are added to the MIP. Inter-rule restrictions can be specified as convex or linear (continuous or discrete) inequalities. Constraint satisfaction is achieved in the final Master-MIP when we reimpose the binary restrictions on z .

Imposing this constraint limits the achievable revenue gain while generating a grading policy that preserves the existing price characteristics of each locality. The decision rules no longer upgrade all houses but contain a mixture of upgrades, downgrades, or no changes based on the living area, age, and number of baths and yields a predicted revenue gain of 9.74%.

In the second constrained scenario which bears some resemblance to a portfolio rebalancing case, we assume the cost of an upgrade is taken as 70% of the predicted sales price increase along with a similar cost saving by downgrading. No cost is incurred for leaving the grade unchanged. The goal is to generate no more than 8 decision rules for grades such that the net cost increase from all the grade changes globally is close to zero. This requirement is practically enforced by limiting the net cost change to less than 1% of the baseline cost (taken as 70% of the predicted sales prices at the original grades). The resulting rules when scored on the test data set yields a predicted revenue gain of 7.82%. The rules essentially rationalize the grades with respect to the predicted return on investment and recommend diverse upgrades and downgrades primarily based on the aggregate living area of the house.

Airline pricing use case

The dataset has more than 1.3×10^6 samples of buy and no-buy data spanning several markets containing more than 10 different multi-level categorical features, and 15 price points on a price grid to choose from. An example of an acceptable rule may look like the following: “if the flight is between Airports A and B, and the ticket was purchased less than 7 days before departure, and the departure time is on a weekday before 11am, then a price of \$400 is prescribed”. The column generation algorithm was run in two modes. In the first mode, we ignored capacity constraints and achieved a overly high predicted revenue gain that was within 12% of the upper bound (UB) obtained by identifying an optimal personalized price rule for every transaction. Note that these personalized prescriptions potentially charge different prices for different customers who buy a ticket at the same time, which violates the user-acceptance requirements. The unconstrained policy satisfies this requirement but creates other operational problems.

Analysis revealed that the unconstrained gain can only be achieved by selling more than twice the number of tickets being sold currently, which is dramatically higher than the available capacity. Airline travelers are price sensitive, and conversion rates are quite sensitive to price changes (e.g., a 10% price cut can result in a 25% increase in conversions for some customer segments). If such rules are deployed it will allow leisure travelers who book early to grab premium seats at a steep

bargain, which in turn can result in early stock-outs. Premium seats will become unavailable to high value travelers who book later and drive them toward competitor airlines in that market. By adding carefully calibrated market-specific constraints on the teacher-model predicted conversions at different prices, we are able to re-optimize the rules satisfactorily and still achieve a predicted gain of more than 25% that is more likely to be realized in live testing compared to the unconstrained policy.

In terms of runtime performance for this challenging constrained setting, the CG iterations converged in about 45 minutes, while the final MIP with the complicating market-specific capacity constraints was solved using the CPLEX solver in a few hours. As the available capacities can change periodically, the model can be warm-started from its most recent solution to quickly re-optimize the decision rules on demand.

References

- Maxime Amram, Jack Dunn, and Ying Daisy Zhuo. Optimal policy trees. *arXiv preprint arXiv:2012.02279*, 2020.
- Mokhtar S Bazaraa, John J Jarvis, and Hanis D Sherali. *Linear programming and network flows*. John Wiley & Sons, 2008.
- Dimitris Bertsimas, Jack Dunn, and Nishanth Mundru. Optimal prescriptive trees. *INFORMS Journal on Optimization*, 1(2):164–183, 2019.
- Max Biggs, Wei Sun, and Markus Ettl. Model distillation for revenue optimization: Interpretable personalized pricing. In *International Conference on Machine Learning*, pages 946–956. PMLR, 2021.
- IBM CPLEX. Introducing ibm ilog cplex optimization studio 20.1.0. <https://www.ibm.com/docs/en/icos/20.1.0>, 2020. Accessed: 2021-03-25.
- GJ Horne. Finding the k least cost paths in an acyclic activity network. *Journal of the Operational Research Society*, 31(5):443–448, 1980.
- Guolin Ke, Qi Meng, Thomas Finley, Taifeng Wang, Wei Chen, Weidong Ma, Qiwei Ye, and Tie-Yan Liu. Lightgbm: A highly efficient gradient boosting decision tree. In *Advances in neural information processing systems*, pages 3146–3154, 2017.
- Scott M Lundberg and Su-In Lee. A unified approach to interpreting model predictions. In *Advances in neural information processing systems*, pages 4765–4774, 2017.